Colloids and Surfaces B: Biointerfaces 163 (2018) 379–384

Contents lists available at ScienceDirect

Colloids and Surfaces B: Biointerfaces

journal homepage: www.elsevier.com/locate/colsurfb

Sparks fly between ascorbic acid and iron-based nanozymes: A study on Prussian blue nanoparticles

Wei Zhang[a,b,c], Yang Wu[d], Hai-Jiao Dong[a], Jun-Jie Yin[e], Hui Zhang[e], Hao-An Wu[a], Li-Na Song[f], Yu Chong[e], Zhuo-Xuan Li[a], Ning Gu[a,b,*], Yu Zhang[a,b,*]

[a] State Key Laboratory of Bioelectronics, Jiangsu Key Laboratory for Biomaterials and Devices, School of Biological Science and Medical Engineering, Southeast University, Nanjing 210096, PR China
[b] Collaborative Innovation Center of Suzhou Nano Science and Technology, Southeast University, Nanjing 210096, PR China
[c] The Jiangsu Province Research Institute for Clinical Medicine, The First Affiliated Hospital with Nanjing Medical University, Nanjing 210029, PR China
[d] Research Centre of Clinical Oncology, Jiangsu Cancer Hospital, Nanjing 210009, PR China
[e] Division of Analytical Chemistry, Office of Regulatory Science, Center for Food Safety and Applied Nutrition, US Food and Drug Administration, College Park, MD 20740, USA
[f] Department of Radiology, Affiliated Hospital of Nanjing University of Chinese Medicine, Nanjing 210029, PR China

ARTICLE INFO

Article history:
Received 29 July 2017
Received in revised form 2 December 2017
Accepted 9 January 2018
Available online 11 January 2018

Keywords:
Prussian blue nanoparticles
Ascorbic acid oxidase
Peroxidase
Electron spin resonance
Anti-cancer efficiency

ABSTRACT

Herein we reported Prussian blue nanoparticles (PBNPs) possess ascorbic acid oxidase (AAO)- and ascorbic acid peroxidase (APOD)-like activities, which suppressed the formation of harmful H_2O_2 and finally inhibited the anti-cancer efficiency of ascorbic acid (AA). This newly revealed correlation between iron and AA could provide new insight for the studies of nanozymes and free radical biology.

1. Introduction

Ascorbic acid (AA) was found very early to be able to induce cancer cell death via improving the intracellular reactive oxygen species (ROS) level [1,2]. Mechanism researches showed high-dose AA treatment induces ROS increment in cancer cells via the auto-oxidation of AA (Eqs. (1) and (2)) and the enhanced cellular uptake dehydroascorbic acid (DHA), the former generate by-product H_2O_2, while the latter can oxidize intracellular reduced enzymes during its reduction [3–5]. As shown in Eqs. (3)–(5), iron is considered to be able to reinforce the anti-cancer effect of AA via Fenton reaction, which is the name given to the reaction of hydrogen peroxide and a ferrous iron catalyst [6].

$$2AA + O_2 \rightarrow 2AA\cdot^- + H_2O_2 \quad (1)$$

$$2AA\cdot^- + O_2 \rightarrow 2DHA + H_2O_2 \quad (2)$$

$$Fe^{2+} + H_2O_2 \rightarrow Fe^{3+} + \cdot OH + OH^- \quad (3)$$

$$Fe^{3+} + H_2O_2 \rightarrow Fe^{2+} + \cdot OOH + H^+ \quad (4)$$

$$AA + Fe^{3+} \rightarrow AA\cdot^- + Fe^{2+} \quad (5)$$

In good agreement with the data from other literatures [7,8], we found iron oxide nanoparticles (IONPs) greatly strengthened the anti-cancer efficiency of AA in 4T1 and MCF7 cells. However, as an iron-based nanomaterial, Prussian blue nanoparticles (PBNPs) inhibited the anti-cancer effect of AA. Further experiments suggested PBNPs reduced the intracellular ROS level while IONPs increased the ROS level in the cells incubated with AA. In our previous studies [9,10], we reported that PBNPs are biologically active as antioxidants because of their peroxidase-, catalase- and superoxide dismutase-like activities arising from their electron transfer ability. Therefore, we inferred PBNPs may play as an AA-related nanozyme, which can catalyze the oxidation of AA without producing H_2O_2.

Ascorbyl radical ($AA^{\bullet -}$) is an intermediate having 10 min half-life formed during the oxidation of AA and this radical can be directly detected by electron spin resonance (ESR) method. ESR

* Corresponding authors at: State Key Laboratory of Bioelectronics, Jiangsu Key Laboratory for Biomaterials and Devices, School of Biological Science and Medical Engineering, Southeast University, Nanjing 210096, PR China.
E-mail addresses: guning@seu.edu.cn (N. Gu), zhangyu@seu.edu.cn (Y. Zhang).

https://doi.org/10.1016/j.colsurfb.2018.01.010
0927-7765/

measurements showed PBNPs can catalyze the oxidation of AA in the absence and presence of H_2O_2, indicating PBNPs possess ascorbic acid oxidase (AAO)-like activity besides ascorbic acid peroxidase (APOD)-like activity. AAO and APOD are both ROS-scavenging enzymes in plants, thus PBNPs may play as ROS-scavenging enzymes in the presence of AA in mammalian cells. Our study show iron plays different roles in different chemical environments such as in PBNPs and IONPs. Certainly, more specific explanation of these phenomena should be given with more exploration.

2. Experimental section

2.1. Reagents and materials

All chemicals used in this experiment were of analytical reagent grade. Deionized water was used throughout the study. Dimercaptosuccinic acid (DMSA) was purchased from Shanghai Zhuorui Chemical Co., Ltd. (Shanghai, China). Polyvinyl pyrrolidone (PVP), hydrogen peroxide (30%) and terephthalic acid (TA) was purchased from Aladdin Co., Ltd. (Shanghai, China). $FeCl_3{\cdot}6H_2O$, $FeSO_4{\cdot}7H_2O$, $K_4[Fe(CN)_6]{\cdot}3H_2O$, ammonia water, oleic acid (OA), ethanol, *n*-haxane and dimethylsulfoxide (DMSO) were purchased from Sinopharm Chemical Reagent Co., Ltd. (Shanghai, China). Tert-butyl alcohol (TBA) was obtained from Shanghai Lingfeng Chemical Reagent Co., Ltd. (China). Ascorbic acid (AA) was obtained from Xilong Scientific Co., Ltd. (Shantou, Guangdong, China). Spin label 3-carbamoyl-2, 2, 5, 5-tetramethyl-3-pyrroline-1-yloxyl(CTPO, ≥98%)was obtained from Radical Vision (Marseille, France). Fetal bovine serum (FBS) and the RPMI 1640 cell culture medium were purchased from Thermo Fisher Scientific (Waltham, MA, USA). 2′,7′-Dichlorodihydrofluorescein diacetate (DCFH-DA), 3,3′,5,5′-Tetramethylbenzidine (TMB), nitroblue tetrazolium (NBT), and 3-(4,5-dimethylthiazole-2-yl)-2,5-diphenyltetrazolium bromide (MTT) were purchased from Sigma-Aldrich (St. Louis, MO, USA). The murine breast cancer cell line 4T1 and the human breast cancer cell line MCF7 were obtained from the American Type Culture Collection (ATCC, Manassas, VA, USA).

2.2. Synthesis of Prussian blue nanoparticles (PBNPs) and iron oxide nanoparticles (IONPs)

PBNPs and IONPs were prepared according to our previous reported works [9,11]. Briefly, PBNPs were prepared by adding 20 mL of $K_4[Fe(CN)_6]{\cdot}3H_2O$ (0.1 mmol) to a 80 mL mixture of $FeCl_3{\cdot}6H_2O$ (0.1 mmol) and PVP (K-30, 10 mmol in terms of monomer) in water with vigorously stirring at 60 °C [12]. A microscale injection pump (WZS-50F6, Smiths Medical) was used to accurately control the adding speed at 40 mL/h. The reaction was kept for 30 min before cooled to room temperature under ambient condition. The dialysis was carried out using a MILLIPORE TTF system (Tangential flow filtration system, MWCO: 130 kDa) in order to exclude remaining impurity ions. The dialyzed solution was then filtrated with 220 nm filter to remove a small quantity of aggregates. To prepare IONPs, 28 g of $FeCl_3{\cdot}6H_2O$ and 20 g of $FeSO_4{\cdot}7H_2O$ were dissolved in 80 mL of deoxygenized water by bubbling nitrogen and heated to in a 72 °C water bath. 40 mL of ammonia water was added under vigorously stir, 9 mL of OA was added 5 min later and continued to stir for 3 h. Next, remove the ammonia water at 85 °C and then cooled to room temperature, removed the impurities by magnetic separation and ethanol lavation and dissolved the product in *n*-hexane. 100 mL of Fe_3O_4@OA solution (4 mg/mL, in *n*-hexane) was mixed with 100 mL of DMSA solution (2 mg/mL, in acetone). Then reflux condensation was conducted at 60 °C. Finally, the product was washed with pure water and dissolved in water, pH was adjusted to 10. Dialyze the solution at pH 7 and the dialyzed solution was then filtrated with 220 nm filter and reserved at 4 °C. The concentration of PBNPs was determined based on a standard curve, which was set up according to the absorbance values at 710 nm of samples of known concentrations prepared by freeze-dried PBNPs powder and calculated by the thermogravimetric analysis.

2.3. Characterization of PBNPs

The particle morphology of the PBNPs and IONPs obtained above were characterized by transmission electron microscopy (TEM, JEOL JEM-2100) with a working voltage of 200 kV.

2.4. Determination of cell viability

MTT method was used to evaluate the cytotoxicity and estimated IC_{50} (half maximal inhibitory) of AA. 4T1 and MCF7 cells were added into each well in a 96-well plate and incubated for 24 h. The culture medium was replaced by fresh medium containing different concentrations of AA, PBNPs and/or IONPs and exposed for 24 h. After washing the cells with serum-free medium, 20 μL of 5 mg/mL MTT solution in PBS-serum free medium was added to each well and incubated for 4 h. Finally, DMSO was added and the optical density (OD) was measured at 570 nm with a microplate reader (Model 680, BIO-RAD, USA) after a 4 h-incubation. Background values of PBNPs and IONPs were deducted, which were counted as the OD at 570 nm of the cells incubated with 150 μL serum-free medium without MTT solution.

2.5. Detection of ROS

4T1 and MCF7 cells were added into 35 mm dishes and incubated for 24 h. The culture medium was replaced by fresh medium containing different concentrations of AA in the presence and absence of PBNPs or IONPs and exposed for 24 h. The concentration of AA and nanoparticles in MCF7 cells were 5 mM and 5 μg(iron)/mL, respectively, while 4T1 cells were cultivated with 0.2 mM AA and 5 μg(iron)/mL nanoparticles. The cells were collected and counted by a cell counting machine (Cellometer Auto 1000, Nexcelom Bioscience, USA).

Intracellular ROS levels were evaluated using the oxidant-sensitivity dye DCFH-DA as probe in a flow cytometry (BD FACS, USA) with fluorescence intensity excited at 488 nm and recorded at 525 nm. Each sample containing 5 million viable MCF7 or 4T1 cells was incubated in 1 mL 1640 serum-free medium with 10 μM DCFH-DA at 37 °C for 20 min in dark. Next, the cells were then washed with PBS three times to thoroughly remove extracellular probe.

The hydroxyl radical (•OH) level was assessed using TA, a very specific detector of hydroxyl radicals [13–16]. TA reacts with •OH to form fluorescent hydroxyterephthaacid (HTA). 1 mL of 2 mM TA solution diluted with 50 mM phosphate buffer (pH 7.5) was added into each sample containing 3 million cells and incubated in dark for 30 min. The fluorescence of each solution was measured using a multimode reader (Infinite 200 PRO, TECAN, Switzerland) with an excitation and emission wavelengths of 315 and 425 nm, respectively.

The superoxide anion ($O_2^{\bullet -}$) content was measured by NBT [17–19]. Firstly, 0.5 mg/mL NBT solution was prepared by dissolving 50 mg of NBT power in 100 mL of PBS buffer (pH 7.4) and filtered with a 0.22 μm filter (Millipore Express). Secondly, 1 mL of NBT solution described earlier was added into each sample containing 1 million cells and incubated at 37 °C for 30 min. Finally, the solutions were centrifuged at 1000 rpm for 5 min and the precipitations were dissolved in DMSO and the OD at 560 nm was measured with a multimode reader (Infinite 200 PRO, TECAN, Switzerland).

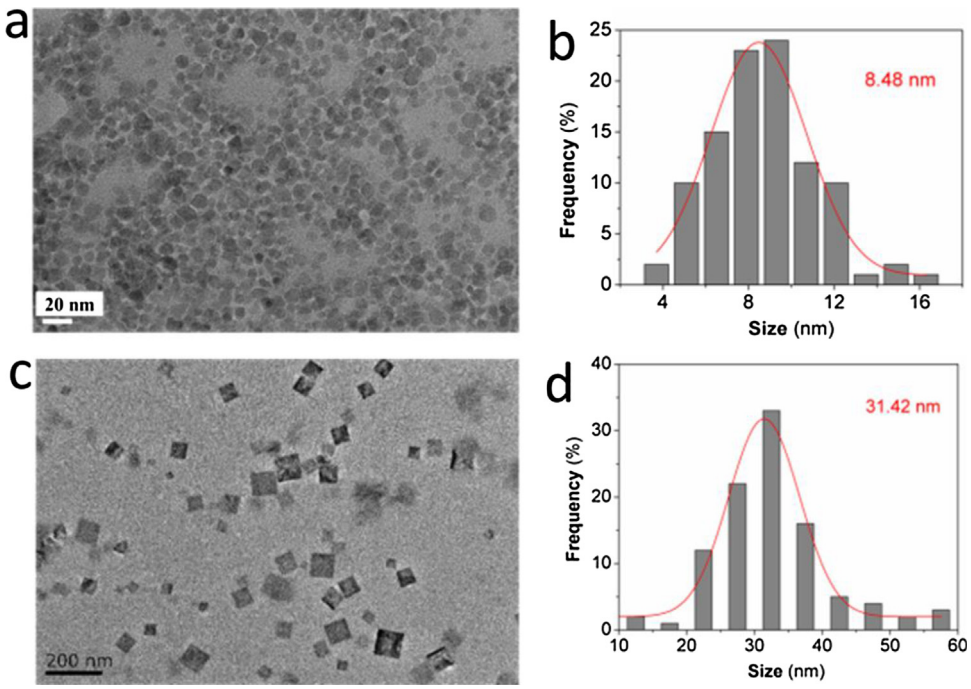

Fig. 1. Characterizations of IONPs and PBNPs. (a) TEM image of IONPs, (b) size distribution of IONPs, (c) TEM image of PBNPs and (d) size distribution of PBNPs.

In pH 3.6 buffer, 0.4 mg/mL TMB, 1.2 M H_2O_2, 0.1 μg[Fe]/mL PBNPs or IONPs were reacted in the presence and absence of TBA. The absorbance (at 650 nm for TMB [20]) of the color reaction was recorded at a certain reaction time via a Microplate Reader (BIO-RAD model 680) to express the generation of •OH

2.6. Detection of ascorbyl radical ($AA^{\bullet-}$) by electron spin resonance (ESR) method

To detect the APOD- and AAO-like activities of PBNPs, ESR was used to record the $AA^{\bullet-}$ signals in pH 7.4, 5.0 and 3.9 buffer solutions. Sample solutions contained different concentrations of AA and PBNPs in the presence or absence of H_2O_2. ESR spectra of $AA^{\bullet-}$ were recorded under the following instrumentation conditions: microwave power 20 mW; field modulation 1 G; sweep width 30 G.

2.7. Detection of oxygen content

ESR oximetry was chosen to monitor the oxygen content of the reaction system.[9] Oxygen concentrations were thus obtained by the ESR spectra of spin label CTPO. PBNPs, AA and H_2O_2 were mixed in a buffer solution of pH 7.4, and then CTPO was used to trap the proton super hyperfine interaction. Sample solutions contained 0.1 mM CTPO, 5 mM AA, 10 mM PBS (pH 7.4), 5 mM H_2O_2 and 500 μM PBNPs. ESR spectra were recorded under the following instrumentation conditions: microwave power 1 mW; field modulation 0.04 G; sweep width 5 G. The AAO-like activity detection of PBNPs was also carried out at room temperature by direct measurement of the oxygen content using a specific oxygen electrode on a Multi-Parameter Analyzer (DZS-708, Cany Precision Instruments Co., Ltd). 5 mM AA, 10 mM PBS (pH 7.4), 5 mM H_2O_2 and 500 μM PBNPs were mixed and the O_2 solubility (unit: mg/L) was measured at different reaction time (0, 2.5, 5, 7.5, 10, 12.5, 15, 17.5, 20 min).

3. Results and discussion

PBNPs and IONPs were prepared according to earlier described methods and characterized using TEM (Fig. 1). The average sizes of IONPs and PBNPs were calculated to be approximately 8.5 nm and 31.4 nm, respectively. Before formal experiments, possible cytotoxicity of IONPs and PBNPs had been checked and half maximal inhibitory (IC_{50}) of AA to MCF7 and 4T1 cells was measured. The cell viability results (Fig. S1) showed IONPs and PBNPs have no significant cytotoxicity to 4T1 and MCF7 cells at concentrations below 12.5 μg(iron)/mL. IC_{50} values for 24 h of AA treatment of MCF7 and 4T1 cells were 5.13 mM and 0.22 mM, respectively (Fig. S2). As shown in Fig. 2a and b, 5 mM and 0.2 mM of AA can remarkably harm the MCF7 and 4T1 cells, leading to ca. 55% of cell viability if AA is used alone. When 5 mM AA was added to the culture medium in the presence of 1.25 μg(iron)/mL IONPs, the MCF7 cell viability was dramatically decreased ($p < 0.05$). Moreover, a successive increase in the concentration of IONPs induced escalating cytotoxicity. However, the addition of PBNPs made the opposite impact. From the free radical biology perspective, we hypothesized the different effects of IONPs and PBNPs could be attributed to their different roles in the AA-mediated production of ROS. Intracellular ROS (Fig. 2c and d) suggested IONPs do play as a peroxidase-like enzyme [21], which enhanced the generation of •OH when exposed to the oxidative stress environment induced by AA, leading to an enhanced cytotoxicity to 4T1 and MCF7 cells in a dose-dependent manner. Moreover, the intracellular $O_2^{\bullet-}$ and •OH levels were determined by NBT and TA, respectively. The results (Fig. S3a) show •OH level was significantly elevated by IONPs ($p < 0.05$).

However, PBNPs do function as an antioxidant in the same oxidative stress environment (Fig. 2c, d and S3). The function of IONPs was thought to be induced by Fenton reaction and the mechanism of PBNPs does need further exploration [21–23]. To further verify the role of •OH, •OH trapping agent was introduced to the pH 3.6 buffer systems containing TMB, H_2O_2 in the presence of PBNPs or IONPs. It can be seen from the results (Fig. S4) that unlike IONPs, the peroxidase-like activity of PBNPs did not exert via the generation •OH generation, consistent with our earlier data [21].

To further study the reaction of PBNPs, H_2O_2 and AA, ESR was used to monitor the intermediate products. As shown in Scheme 1, $AA^{\bullet-}$ is a free radical generated during the oxidation of AA, which can be directly recorded by ESR. As shown in Fig. 3, the $AA^{\bullet-}$ sig-

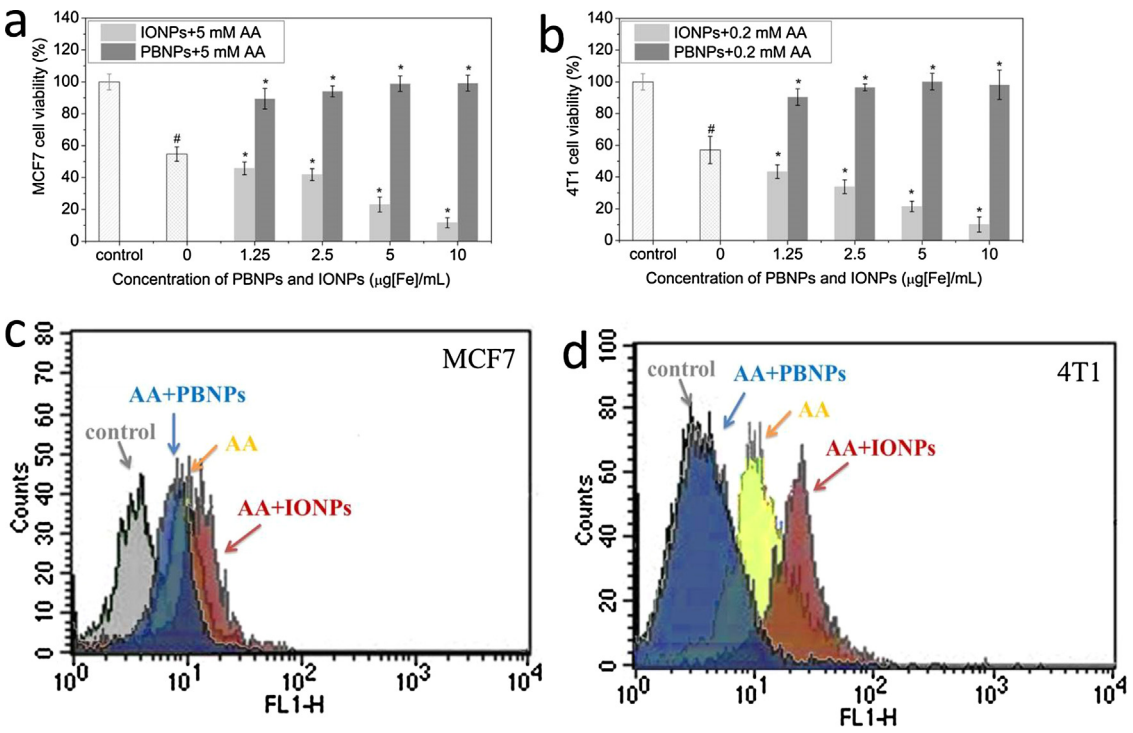

Fig. 2. Effects of the concentration of IONPs and PBNPs on MCF7 (a) and 4T1 (b) cell viability with treatment of 5 mM and 0.2 mM AA, respectively. The data were normalized to control values (no particle and AA exposure), which were set as 100% cell viability; # indicates $p < 0.05$ as compared with control group and * indicates $p < 0.05$ as compared to AA group (no particle exposure), mean SEM, n = 5. Treated MCF-7 (c) and 4T1 (d) cells were assessed for intracellular ROS generation by measuring DCF-fluorescence and analyzed by a flow cytometer. The concentration of AA and nanoparticles in MCF7 cells were 5 mM and 5 μg(iron)/mL, respectively, while 4T1 cells were cultivated with 0.2 mM AA and 5 μg(iron)/mL nanoparticles.

$$2AA\cdot^{-} + H_2O_2 \xrightarrow{PBNPs/APOD} 2DHA + 2H_2O \qquad (7)$$

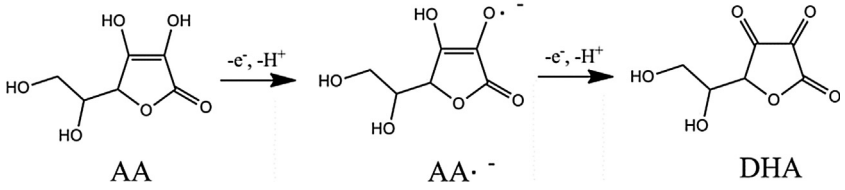

Scheme 1. Oxidation of AA in the presence of O_2 and catalyzed by AAO.

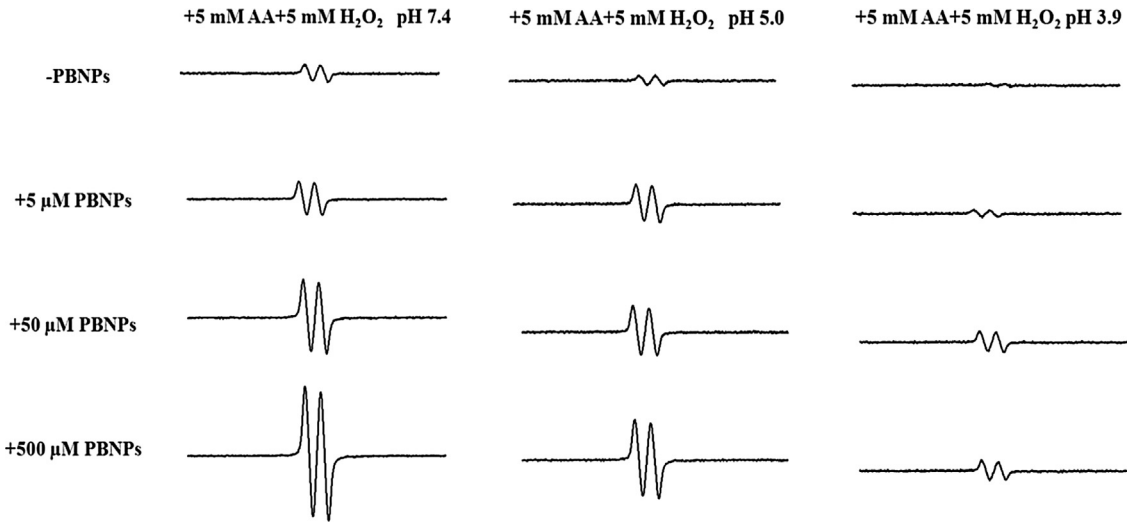

Fig. 3. APOD-like activity of PBNPs detected by ESR spectrum of the ascorbyl radical. Sample solutions contained 5 mM AA, buffers (pH 7.4, 5.0, 3.9), 5 mM H_2O_2 and different concentrations of PBNPs. ESR spectra were collected at 1 min after sample mixing.

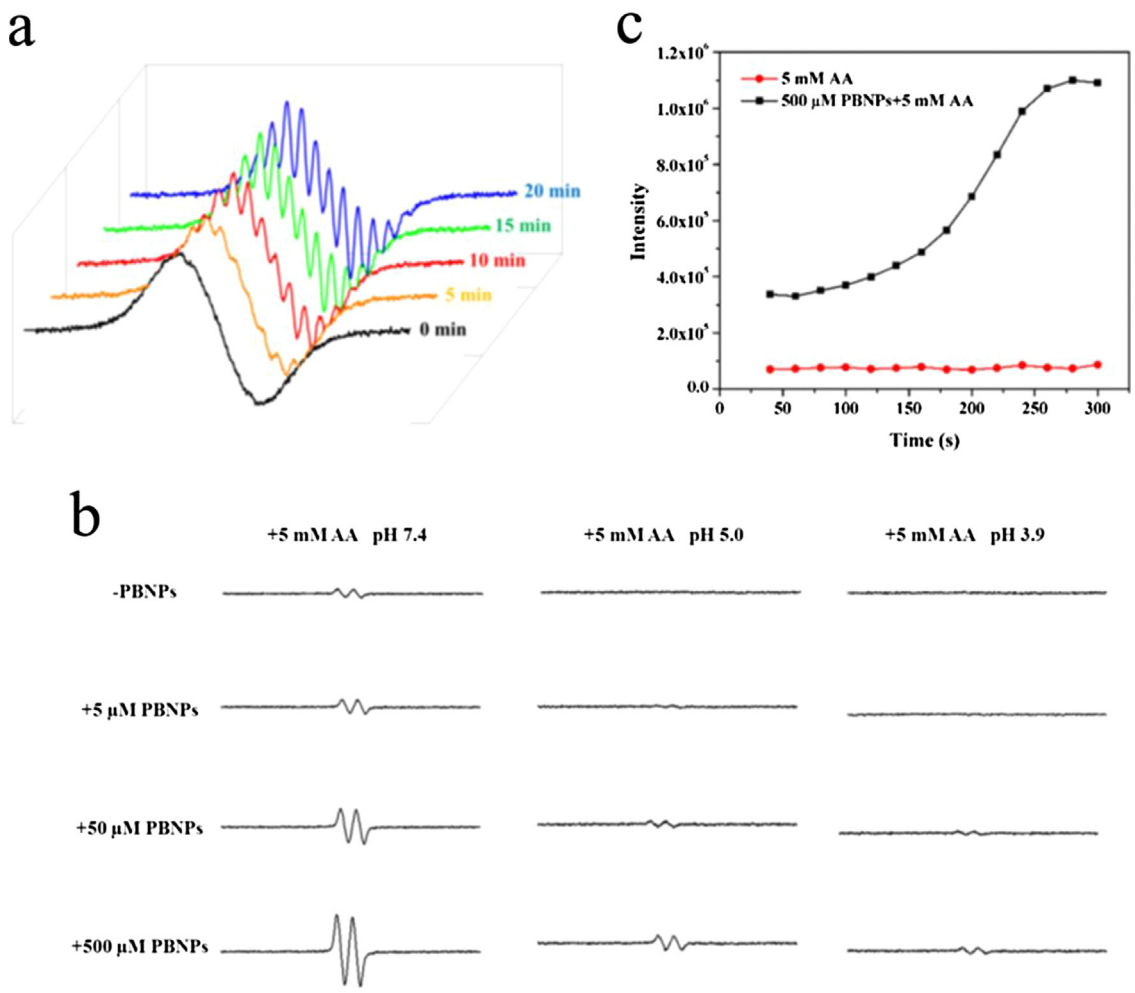

Fig. 4. AAO-like activity of PBNPs. (a) ESR spectrum of the spin label CTPO during the oxidation of AA catalyzed by PBNPs. Sample solutions contained 0.1 mM CTPO, 5 mM AA, 10 mM PBS (pH 7.4) and 500 μM PBNPs. ESR spectra were obtained at 0, 5, 10, 15 and 20 min after addition of PBNPs. (b) AAO-like activity of PBNPs detected by ESR spectrum of the ascorbyl radical. Sample solutions contained 0.1 mM CTPO, 5 mM AA, 10 mM PBS (pH 7.4) and 50 μM PBNPs. (c) The signal intensity was measured as the peak-to-peak value of the first line of the spectrum. ESR spectra were collected at 1 min after sample mixing.

nals in reaction solutions without PBNPs (-PBNPs groups) indicate the auto-oxidation of AA is quite slow. Comparing the signals of $AA^{\bullet -}$ in pH 7.4, 5.0 and 3.9 buffer solutions, we can conclude that PBNPs catalyzed the oxidation of AA by H_2O_2. Moreover, the $AA^{\bullet -}$ signal intensity was positively associated with the concentration of PBNPs and the pH levels. Meanwhile, the data in Fig. S5 show there is also a positive correlation between the $AA^{\bullet -}$ signal intensity and AA concentration. These results further verify that PBNPs are peroxidase mimics taking AA as substrate (Eqs. (6) and (7)).

$$2AA + H_2O_2 \overset{PBNPs/APOD}{\rightarrow} 2AA\cdot^{-} + 2H_2O \quad (6)$$

$$2AA\cdot^{-} + H_2O_2 \overset{PBNPs/APOD}{\rightarrow} 2DHA + 2H_2O \quad (7)$$

As shown in our previous study, PBNPs possess catalase-like activity (Eq. (8)) at pH 7.4 [9]. In this study, we monitor the oxygen content in pH 7.4 reaction system to investigate the catalase-like activity of PBNPs. CTPO is quite sensitive to oxygen concentration, thus ESR oximetry was usually used to monitor the small variations of oxygen concentration [9,24]. Less evident resolution of the super hyperfine structure of the low-field line of ESR spectra of CTPO represents higher oxygen concentration. As shown in Fig. 4a, at pH 7.4, the resolution of super hyperfine structure of CTPO in the solution containing AA and PBNPs gradually became evident in 20 min, indicating the consumption of O_2 in a closed capillary. Similarly, as shown in Fig. S6, the oxygen content as also monitored by a specific oxygen electrode and the results verify the consumption of O_2.

$$2H_2O_2 \overset{PBNPs/catalase}{\rightarrow} 2H_2O + O_2 \quad (8)$$

$$2AA + O_2 \overset{PBNPs/AAO}{\rightarrow} 2AA\cdot^{-} + H_2O_2 \quad (9)$$

$$2AA\cdot^{-} + H_2O_2 \overset{PBNPs/APOD}{\rightarrow} 2DHA + 2H_2O \quad (10)$$

The disappearance of oxygen in solution during oxidation of AA catalysed by PBNPs hints PBNPs may catalyse the oxidation of AA by oxygen. ESR signal intensity of $AA^{\bullet -}$ (Fig. 4b) in the reaction solution contained only AA and PBNPs (without H_2O_2) is dependent on the concentration of PBNPs, with the strongest signal at pH 7.4. The amount of $AA^{\bullet -}$ in the pH 7.4 solution reaches a plateau 300 s later while the auto-oxidation of AA is quite slight during 300 s (Fig. 4c). The reaction process of AAO-like activity can be expressed by Eqs. (9) and (10). Altogether, PBNPs can catalyze reactions consuming H_2O_2 due to their APOD and AAO-like activities, which subsequently lead to the protective effect on MCF7 and 4T1 cells from the killing of AA.

4. Conclusions

In conclusion, we demonstrated that PBNPs possess APOD- and AAO-like activities. The results of cellular experiment taking AA as

a model molecule show iron plays different roles when placed in the different chemical environments of PBNPs and IONPs. These data provide new insights in the study of iron-based enzymes and iron-based nanomaterials.

Conflict of interest

The authors declare no competing financial interest.

Acknowledgements

This research was supported by the National Key Research and Development Program of China (No. 2017YFA0205502), the National Basic Research Program of China (973 program No. 2013CB733800), National Natural Science Foundation of China (No. 81571806, 81671820, 81301870), the Jiangsu Provincial Special Program of Medical Science (No. BL2013029), the Fundamental Research Funds for the Central Universities. This work was also partially supported by a regulatory science grant under the FDA Nanotechnology CORES Program. This paper is not an official US FDA guidance or policy statement. No official support or endorsement by the US FDA is intended or should be inferred.

Appendix A. Supplementary data

Supplementary data associated with this article can be found, in the online version, at https://doi.org/10.1016/j.colsurfb.2018.01.010.

References

[1] C.M. Doskey, V. Buranasudja, B.A. Wagner, J.G. Wilkes, J. Du, J.J. Cullen, G.R. Buettner, Tumor cells have decreased ability to metabolize H2O2: implications for pharmacological ascorbate in cancer therapy, Redox Biol. 10 (2016) 274–284.
[2] F. Li, L. Zhang, S.-C. Tang, Revisiting vitamin C in cancer therapy: is C for cure or just wishful thinking? Genes Dis. 3 (2016) 1–2.
[3] S.-A. Jung, D.-H. Lee, J.-H. Moon, S.-W. Hong, J.-S. Shin, I.Y. Hwang, Y.J. Shin, J.H. Kim, E.-Y. Gong, S.-M. Kim, E.Y. Lee, S. Lee, J.E. Kim, K. -p. Kim, Y.S. Hong, J.S. Lee, D.-H. Jin, T. Kim, W.J. Lee, L-Ascorbic acid can abrogate SVCT-2-dependent cetuximab resistance mediated by mutant KRAS in human colon cancer cells, Free Radic. Biol. Med. 95 (2016) 200–208.
[4] J. v. d. Reest, E. Gottlieb, Anti-cancer effects of vitamin C revisited, Cell Res. 26 (2016) 269–270.
[5] J. Yun, E. Mullarky, C.Y. Lu, K.N. Bosch, A. Kavalier, K. Rivera, J. Roper, I.I.C. Chio, E.G. Giannopoulou, C. Rago, A. Muley, J.M. Asara, J. Paik, O. Elemento, Z.M. Chen, D.J. Pappin, L.E. Dow, N. Papadopoulos, S.S. Gross, L.C. Cantley, Vitamin C selectively kills KRAS and BRAF mutant colorectal cancer cells by targeting GAPDH, Science 350 (2015) 1391–1396.
[6] J. Xia, H. Xu, X. Zhang, C. Allamargot, K.L. Coleman, R. Nessler, I. Frech, G. Tricot, F. Zhan, Multiple myeloma tumor cells are selectively killed by pharmacologically-dosed ascorbic acid, EBioMedicine 18 (2017) 41–49.
[7] J.-H. Park, S.-J. Kim, J.-H. Jeong, S.Y. Nam, Y.W. Yun, J.-S. Kim, B.J. Lee, Effect of nano-sized iron overload with ascorbic acid on the formation of colonic pre-neoplastic lesions in mice, J. Prev. Vet. Med. 40 (2016) 83–89.
[8] X.J. Hou, X.P. Huang, Z.H. Ai, J.C. Zhao, L.Z. Zhang, Ascorbic acid/Fe@Fe2O3: A highly efficient combined Fenton reagent to remove organic contaminants, J. Hazard. Mater. 310 (2016) 170–178.
[9] W. Zhang, S. Hu, J.-J. Yin, W. He, W. Lu, M. Ma, N. Gu, Y. Zhang, Prussian blue nanoparticles as multienzyme mimetics and reactive oxygen species scavengers, J. Am. Chem. Soc. 138 (2016) 5860–5865.
[10] W. Zhang, N. Gu, Y. Zhang, Prussian blue nanoparticles possess potential anti-inflammatory properties via scavenging reactive oxygen species, Inflamm. Cell Signal. 3 (2016) e1342.
[11] Y. Wu, M. Song, Z. Xin, X. Zhang, Y. Zhang, C. Wang, S. Li, N. Gu, Ultra-small particles of iron oxide as peroxidase for immunohistochemical detection, Nanotechnology 22 (2011) 225703.
[12] T. Uemura, S. Kitagawa, Prussian blue nanoparticles protected by poly (vinylpyrrolidone), J. Am. Chem. Soc. 125 (2003) 7814–7815.
[13] M. Zhuang, C. Ding, A. Zhu, Y. Tian, Ratiometric fluorescence probe for monitoring hydroxyl radical in live cells based on gold nanoclusters, Anal. Chem 86 (2014) 1829.
[14] Y. Zhu, S. Pei, J. Tang, H. Li, L. Wang, W.Z. Yuan, Y. Zhang, Enhanced chemical durability of perfluorosulfonic acid membranes through incorporation of terephthalic acid as radical scavenger, J. Membr. Sci. 432 (2013) 66–72.
[15] J.C. Barreto, G.S. Smith, N.H.P. Strobel, P.A. Mcquillin, T.A. Miller, Terephthalic acid: a dosimeter for the detection of hydroxyl radicals in vitro, Life Sci. 56 (1994) 89–96.
[16] A. Shanei, M.M. Shanei, Effect of gold nanoparticle size on acoustic cavitation using chemical dosimetry method, Ultrason. Sonochem. 34 (2017) 45.
[17] R. Xing, H. Yu, S. Liu, W. Zhang, Q. Zhang, Z. Li, P. Li, Antioxidant activity of differently regioselective chitosan sulfates in vitro, Biorg. Med. Chem. 13 (2005) 1387–1392.
[18] P. Valembois, M. Lassègues, In vitro generation of reactive oxygen species by free coelomic cells of the annelid Eisenia fetida andrei: an analysis by chemiluminescence and nitro blue tetrazolium reduction, Dev. Comp. Immunol 19 (1995) 195.
[19] L. Gao, J. Zhuang, L. Nie, J. Zhang, Y. Zhang, N. Gu, T. Wang, J. Feng, D. Yang, S. Perrett, X. Yan, Utility of the nitroblue tetrazolium reduction test for assessment of reactive oxygen species production by seminal leukocytes and spermatozoa, J. Androl. 24 (2003) 862–870.
[20] N.H. Kim, M.S. Jeong, S.Y. Choi, J.H. Kang, Peroxidase activity of cytochrome c, Bull. Korean Chem. Soc 25 (2004) 1889.
[21] Z. Chen, J.-J. Yin, Y.-T. Zhou, Y. Zhang, L. Song, M. Song, S. Hu, N. Gu, Dual enzyme-like activities of iron oxide nanoparticles and their implication for diminishing cytotoxicity, Acs Nano 6 (2012) 4001–4012.
[22] X.-Q. Zhang, S.-W. Gong, Y. Zhang, T. Yang, C.-Y. Wang, N. Gu, Prussian blue modified iron oxide magnetic nanoparticles and their high peroxidase-like activity, J. Mater. Chem. 20 (2010) 5110–5116.
[23] L. Gao, J. Zhuang, L. Nie, J. Zhang, Y. Zhang, N. Gu, T. Wang, J. Feng, D. Yang, S. Perrett, Intrinsic peroxidase-like activity of ferromagnetic nanoparticles, Nat. Nanotechnol. 2 (2007) 577–583.
[24] T. Wen, W.G. Wamer, W.K. Subczynski, S. Hou, X. Wu, J.-J. Yin, Enhancement of paramagnetic relaxation by photoexcited gold nanorods, Sci. Rep. 6 (2016) 24101.